

Shape Optimization of Membrane Structures based on Finite Element Simulation

C.W. Lim¹, V.V. Toropov^{1,2} and J. Ye³

¹School of Civil Engineering,

²School of Mechanical Engineering

University of Leeds, United Kingdom

³Department of Engineering, Lancaster University, United Kingdom

Abstract

As a result of the inherently small bending resistance of membrane structures, small compressive stresses inevitably lead to wrinkling that is undesirable for such lightweight structures. This paper reviews several possible formulations of an optimization problem where the nodal out-of-plane displacements are minimized using sequential quadratic programming, a fast and accurate gradient-based optimisation technique. A comparison of several problem formulations is performed on a benchmark problem of finding the optimum shape and thickness of the corner reinforcement patches at which the tension forces are applied to a square membrane. A geometrically nonlinear finite element simulation is performed to find the displacements resulting in wrinkling. The design variables are parameters defining the geometry of the patches as well as their thickness, and the volume of the patch material is constrained. The obtained results are used to provide recommendations on the choice of an approach to the optimisation problem formulation.

Keywords: membrane, finite element simulation, wrinkling, shape optimization, p-mean criterion, sequential quadratic programming.

1 Introduction

Membrane has no ability to sustain any compressive stresses, when exist they are immediately released by wrinkling, an out-of-plane deformation. Wrinkling can occur when a membrane structure is in shear due to boundary displacement, or an in-plane concentrated force is applied. Wrinkling is undesirable for such lightweight structures as it deteriorates the performance and stability of the structure by altering the load path and the structural stiffness of the membrane. For example, it can degrade the surface reflectivity that is a key design parameter for some of the space structures, it modifies dynamic characteristics of membranes and can also cause a

non-uniform surface heating in solar sails. Also, this phenomenon is aesthetically unpleasant for very large-scale structures on the ground, e.g. membrane roofing over airports or stadiums. It is therefore very important to control and minimize the wrinkling of membrane structures.

Even though there have been many experimental as well as numerical studies of wrinkled membranes over the years, the research on the strategies to minimize or suppress the membrane wrinkling still remains limited. Apart from formulating design problems as optimization problems, several *ad hoc* approaches to the problem were investigated in recent years [1, 2]. Shape memory alloy (SMA) wires and electroactive polymers (EAPs) have been used to control wrinkling formation of inflatable booms and membranes. These smart materials behave as actuators by converting electrical energy into mechanical energy in order to improve the bending resistance of membranes and hence control the wrinkling. Such technical solutions can be applicable to some general purpose membrane structures but they remain expensive in both operation and initial cost for large scale structures.

Two other membrane designs approaches to mitigating wrinkles around the edges when the supports at corners are perturbed thus stressing the membrane have been proposed. The first design approach utilizes a shear compliant border where regions along the perimeter are made of thermoformed strips to prevent wrinkles induced by shear from propagating into the central domain of the membrane [3]. The other approach is a so-called web-cable girded design that employs layers of suspension cables around the membrane [4]. The latter design is more mass-efficient as compared to the former. Both designs achieve an almost uniform biaxially pre-stressed state in the membrane but the design process is quite complicated. Another application in which wrinkling control is important is an inflatable antenna reflector. The influences of several design parameters to wrinkling formation of these structures were summarized in [5]. Among those parameters are thickness, structural scale, the magnitude of initial pre-stress and pressure, and the number of tension ribs or gores.

A simpler approach to controlling and minimizing wrinkling on membrane structures using an optimization method was recently introduced in [6]. In that study, the out-of-plane deformation caused by wrinkling is first described by an in-plane contraction. Through this process, the total strain of a partially wrinkled membrane is then decomposed into: (a) an elastic strain, which is equivalent to the material strain due to stretching in the direction of the major principal stress, and (b) geometrical shortening/wrinkling strain induced by a wrinkle. The strain energy density is called in this case wrinkle intensity. This quantity depends only on the wrinkling mode and is the objective function in the optimization problem formulation in that study. The boundary of the finite element model was characterized by a non-uniform rational B-spline (NURBS) curve and the design variables define the curve-passing points. The surface area of the membrane acts as a constraint in this problem formulation.

An investigation into the removal of thermally induced wrinkles to ensure flatness of a membrane structure was carried out in [7]. An adaptive genetic algorithm (AGA) with reweighting of the objective function was developed to search for an optimum tension forces combination which minimizes the wrinkle

amplitude with the flatness estimation performed by a neural network.

More often, in many membrane structures such as solar sails or yacht sails, corner reinforcement patches made of a stiffer material are used for such ultra-thin membrane structures to disperse the stresses at the corners, preventing membrane surface from being overloaded in tension. Among those patch designs, radial patches are common. The shape of these components can determine the wrinkling pattern within the membrane when loaded. In our research the optimum shape of the patches is obtained using numerical optimization. Wrinkled membrane is modelled using shell elements. The objective function is to minimize the amplitude of wrinkles radiating from the corners and the design variables are geometric parameters of the patches. It is a constrained optimization problem where an optimal distribution of a given amount of material is sought. Using the Sequential Quadratic Programming method (SQP), a fast and highly accurate gradient-based optimization method, a series of simulations with different objective function formulations aiming at minimizing the wrinkling of the membrane have been performed. These formulations of the objective function include the root mean square (RMS) of the nodal out-of-plane displacement W , a generalized mean power of the exponent p of W for a range of values of parameter p , the maximum of nodal values of W , and the maximum of $|W|$. The generalized mean power of exponent p , is referred to as p -mean in this paper. Another possible formulation is a minmax formulation where the local maxima of W in different zones are minimized using Olhoff's bound formulation. For the obtained designs a sensitivity study is performed to check whether a design is robust, i.e. whether it is affected by small variations of the design variables. To conclude this paper, all optimization problem formulations are compared to identify the advantages and pitfalls of each and provide practical recommendations to designers of membrane structures.

2 Wrinkled membrane finite element simulation

2.1 Model description

Wrinkling simulation of a membrane was carried out using the commercial finite element software ABAQUS. An FE model of a 500 mm square membrane, assumed to be isotropic with the material properties summarized in Table 1 was created.

Parameter	Membrane	Patches
Young's Modulus, E (N/mm ²)	3530	6500
Thickness, t (μ m)	25	100
Poisson ratio, ν		0.33
Material		Kapton

Table 1: Material properties of wrinkled membrane

Due to the symmetry in geometry, boundary conditions and loading, only a quarter of the finite element model is considered, as shown in Figure 1, to study the

formation of wrinkles radiating from the corner. Two pairs of equal forces F , acting in opposite directions along the diagonals, are applied at the corners. The membrane is pre-stressed by uniformly distributing the corner tensile forces along the patch edges through the patches onto the membrane.

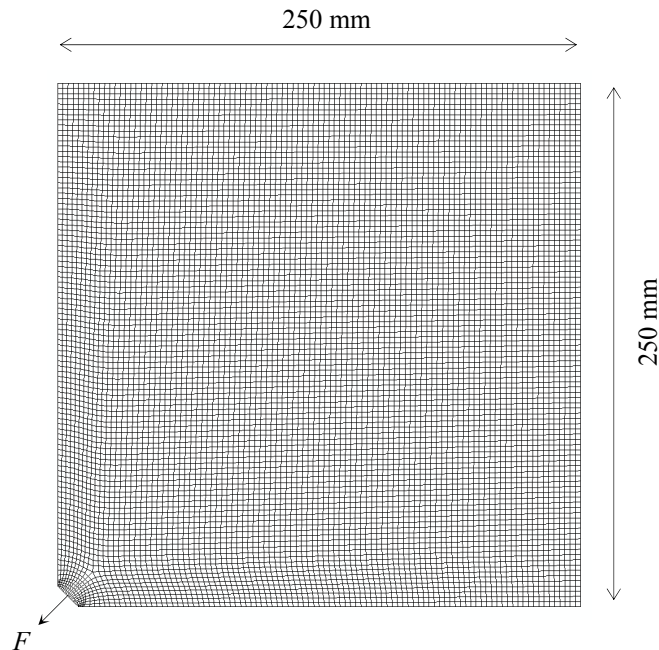


Figure 1: Finite element model (quarter of the membrane)

A high density (100 elements along each symmetry line) mesh of S4R5, 4-node reduced integration with hourglass control, five degrees of freedom per node, thin shell elements was chosen after several preliminary analyses [8], to capture fine wrinkles due to tensile loading at the corners. Symmetric boundary conditions were applied at symmetry lines, i.e. top and right edge of the model in Figure 1, and the other two edges are free. The out-of-plane translational displacement and all rotational degrees of freedom of the nodes along the truncated corner patches were restrained. It should be noted that the corners were truncated to remove the severe stress concentration that would cause numerical instability.

2.2 FE simulation

A pre-stress of sufficient magnitude was first applied to the membrane to successfully steer the subsequent pre-buckling eigenvalue analysis. As the shell elements are thin, their bending stiffness is so small that obtaining meaningful results can be a challenge when in-plane loads are applied. A pre-stress that is not large enough would result in obtaining only negative eigenvalues as well as closely spaced eigenvalues, both of which can cause numerical problems. The negative eigenvalues indicate that the structure would buckle if the loads were applied in the

opposite direction, i.e. a membrane is to buckle when compressive loads replace the tensile loads. The pre-stress was introduced by applying 10 N equal tensile forces applied at the corners in the diagonal directions. A static geometrically nonlinear analysis was used to check the equilibrium of the system, with the ABAQUS input option `NLGEOM = YES` activated.

Next, a buckling analysis (`*BUCKLE`) step was carried out using the Lanczos eigensolver, with minimum eigenvalue of interest set to zero, to extract positive eigenmodes. A perturbation load was defined in this step. The magnitude of this loading pattern is not important, as the aim of the pre-buckling eigenvalue analysis is to provide a reasonable estimate of the wrinkling modes used to seed the geometrical imperfections. Figure 2 shows the first few eigenmodes of the wrinkled membrane.

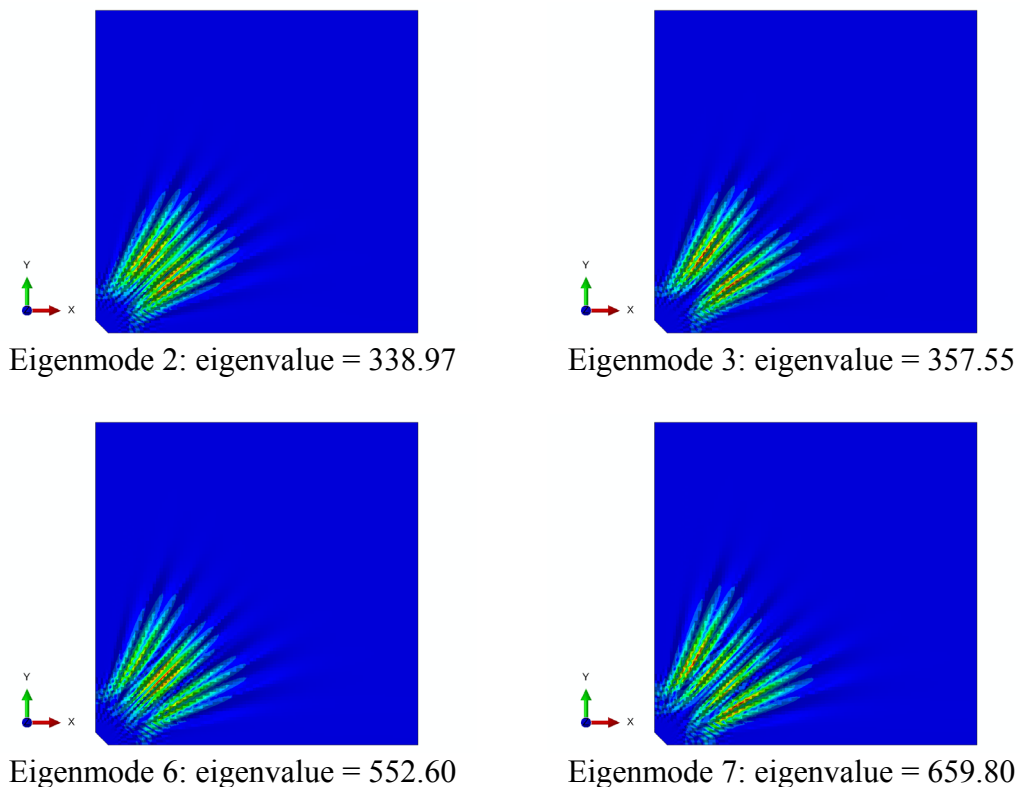


Figure 2: Four symmetric eigenmodes selected as initial geometric imperfection

Finally, a linear combination of the selected eigenmodes was used to introduce geometrical imperfections using the `*IMPERFECTION` keyword to the perfect geometry to create the perturbed mesh for the post-buckling analysis. Each eigenmode was multiplied by a scaling factor that was a few percent of the membrane thickness. An automatically stabilized geometrically non-linear simulation of wrinkles was performed by imposing the `STABILIZE` input option to introduce pseudo-inertia and pseudo-viscous forces at all nodes when an instability is detected, and simulates a possible dynamic response of the structure as it snaps in

order to obtain the first static equilibrium state after snapping has occurred. Instead of continuing with the quasi-static analysis, ABAQUS automatically switches to a dynamic integration of the equations of motion for the structures, thus reducing the likelihood of numerical singularities. The loading pattern in this step is similar to the first step when applying initial pre-stress, but the magnitude was increased to 50 N for simulation of larger wrinkle amplitude.

3 Shape optimization problem

It has been attempted to find the optimum shape of the radial corner reinforcement patches as shown in Figure 3. The baseline design shape of these patches is treated as a quadratic parabola symmetric about the diagonal. Prior to the optimization, it is necessary to investigate the wrinkle patterns as well as the stress distribution of the baseline model due to wrinkling.

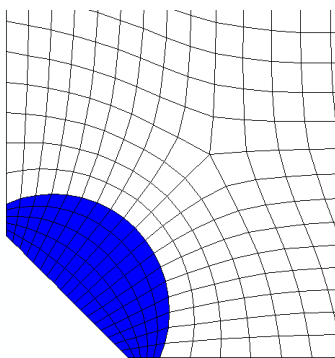


Figure 3: Baseline design of the patches

The reinforcement patches are made of stiffer material and are thicker compared to the membrane. They are bonded to the top and bottom surface of the membrane at each corner. As the objective of this investigation is to establish a methodology of finding an optimum shape of the patches that minimizes the wrinkling of the membrane, the cohesive layers between the patches and membrane have not been modelled. The total nominal thickness of the patches including the membrane is $225 \mu\text{m}$.

Figure 4 shows (a) a contour plot of the out-of-plane displacement W (all values are in mm), and (b) a magnified wrinkling profile at a cross-section corresponding to a distance along the diagonal axis $\zeta = 80 \text{ mm}$ measured from the corner. Figure 5 shows the wrinkling amplitude along the cross-section.

The simulated wrinkles radiate from the corners, as expected. The wrinkling amplitudes were found to be extremely small hence a magnification factor of 10^4 was used to show the wrinkling profile (Figure 4 b). This is due to the fact that a membrane loaded by the equal corner forces is almost flat everywhere except for the regions near the corners where wrinkles form. As seen in Figure 5, the peaks-

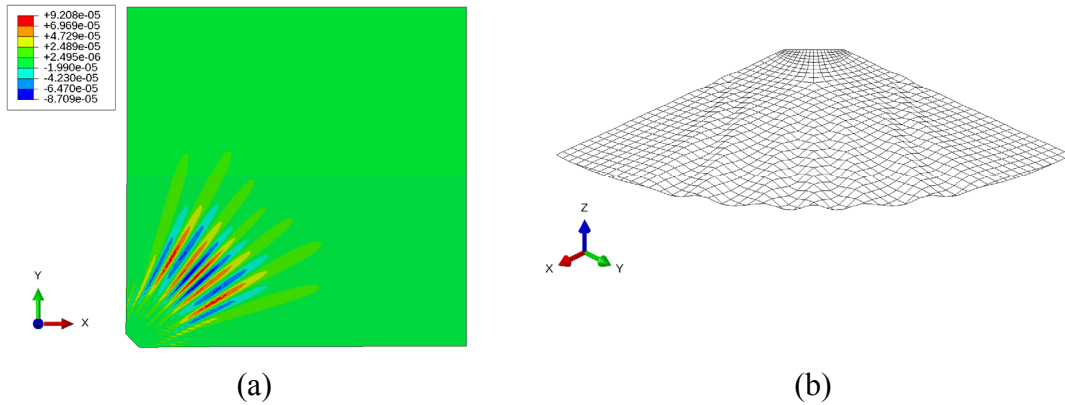


Figure 4: Wrinkle pattern for $F = 50$ N: (a) contour of out-of-plane displacement, and (b) wrinkle profile

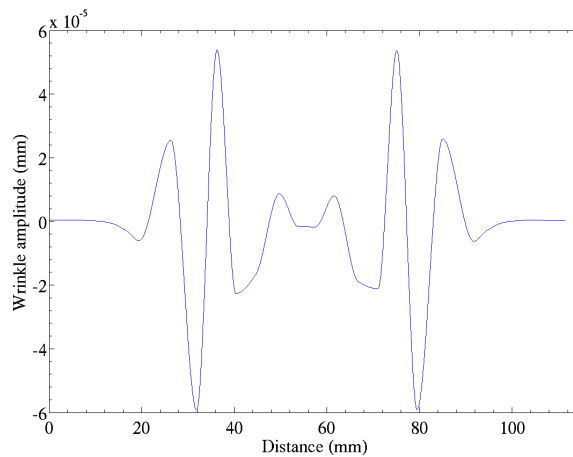


Figure 5: Wrinkling amplitude

troughs and crests of the wrinkles on either side of the membrane are attained which are parallel to the major principal stress direction. The direction of the wrinkles is always perpendicular to the tension lines. Due to the material contraction, larger wrinkles were found at either side from the middle of the cross-section, about three times larger than those in the middle.

The contours in Figure 6 show the principal stress distribution (N/mm^2) in the wrinkled membrane. The major principal stress in most of the membrane surface around the centre is fairly uniform, and is at least an order of magnitude lower than the maximum stresses in the vicinity of the stiffer patches. The patches may have contributed to the higher localised stresses in the model. The negative minor principal stress around the corners of the membrane demonstrates the existence of small compressive stresses which are released by the wrinkles.

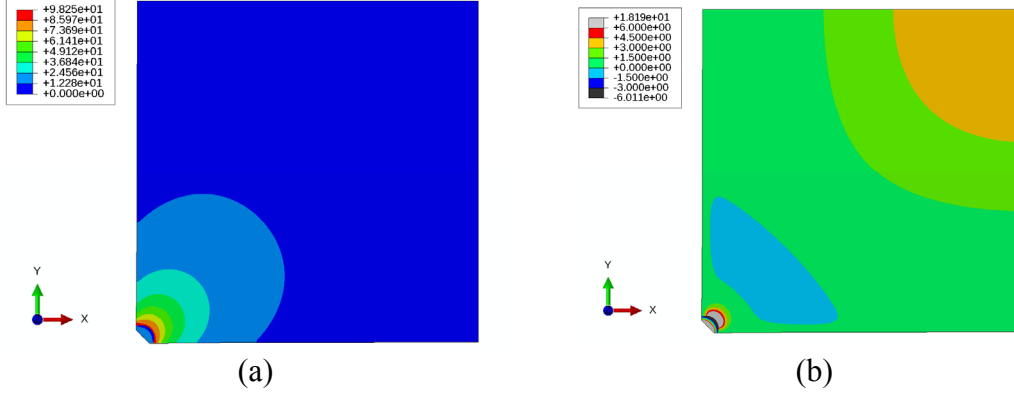


Figure 6: Contours of principal stresses: (a) major principal, and (b) minor principal

3.1 Problem formulation

To determine the optimum shape of the radial corner reinforcement patches the optimization problem is posed as follows:

minimize:

$$f(\mathbf{x}) = f(x_1, x_2, \dots, x_n) \quad (1)$$

subject to:

$$g(\mathbf{x}) = g(x_1, x_2, \dots, x_n) \leq 100\% \quad (2)$$

and

$$x_n^L \leq x_n \leq x_n^U \quad (3)$$

where $x = (x_1, x_2, \dots, x_n)$ is a vector of n design variables that are the thickness and the patch shape variables, x_n^L and x_n^U are the lower and upper bounds of each design variable, and n is the number of design variables. The nominal, lower and upper bounds values of the design variables are listed in Table 2.

Design variables	Description	Nominal	Upper bound	Lower bound
x_1	Thickness (μm)	225	325	125
x_2	Shape factor	0	1.0	-0.5
x_3	Shape factor	0	1.0	-0.5

Table 2: Design variables

The objective function $f(\mathbf{x})$ quantifies the magnitude of the nodal out-of-plane displacement W via the following formulations:

$$f(\mathbf{x})_{max} = \max_N W \quad (4)$$

$$f(\mathbf{x})_{abs} = \max_N |W| \quad (5)$$

$$f(\mathbf{x})_{RMS} = \text{RMS} = \sqrt{\frac{\sum_1^N W^2}{N}} \quad (6)$$

$$f(\mathbf{x})_{p\text{-mean}} = \left[\frac{1}{N} \sum_1^N (W)^p \right]^{\frac{1}{p}} \quad (7)$$

where N is the total number of nodes, p is an even integer number [9].

The constraint function $g(\mathbf{x})$ is the volume of the patches normalised by the baseline patch volume and expressed as percentage (%):

$$g(x) = \frac{(\sum_1^K V)_i}{(\sum_1^K V)_0} \times 100\% \quad (8)$$

where K is the number of finite elements in the model, in other words, the design of the patches results in an optimal distribution of no more than a given amount of material.

Two shape variables were defined by morphing the geometry of the patches, i.e. the parabolic boundary of the domain, using the HyperMorph module in Altair HyperMesh 11.0. Figure 7 illustrates the morphed mesh shapes of the patches done by two operations: (a) curve ratio alteration and (b) handle perturbations.

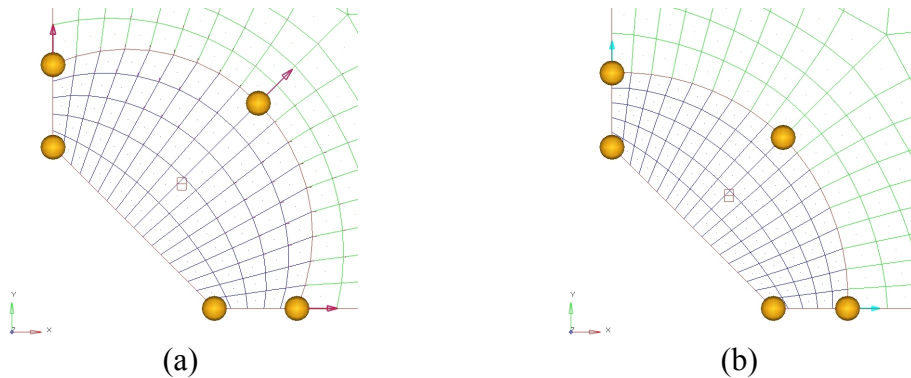


Figure 7: Morphed shape entities: (a) curve ratio alteration, and (b) handle perturbations defined by the shape variables

The so-called local domains and handles approach was chosen to allow this parametric morphing process. The entire model was first divided into local domains containing elements and nodes at different parts, i.e. membrane and patches, and placing handles (orange coloured in Figure 7) at the corners of those domains. When the handles associated with a domain are moved, the shape of the mesh changes following the domain boundary, i.e. nodes at the edge domains move as a function of the handles at the edge domain. In the areas between the handles, the mesh is either stretched or compressed to match the desired shape.

The first shape variable (Figure 7 a) was created by altering the curve ratio of the outer edge domain and increased to the ratio of 1.2 in the centre to that at the corner. Meanwhile, the second shape variable (Figure 7 b) was defined by translating the handles along x and y -axis, i.e. handles with arrows, by 2 mm. These mesh perturbations are “unit” morphed shapes constrained by the lower and upper bound values, i.e. shape factors x_1 for the first shape variable, and x_2 for the second shape variable, as shown in Table 2. The coloured arrows on the handles represent the mesh perturbation direction and magnitude.

For multi-objective optimization (MOO), the minmax method with Olhoff’s bound formulation [10, 11] was adopted to minimize the local maxima of W at different zones as follows:

$$\min \left[\max \left(\frac{f_1(x)}{\bar{f}_1}, \frac{f_2(x)}{\bar{f}_2}, \dots, \frac{f_m(x)}{\bar{f}_m} \right) \right] \quad (9)$$

where m is the number of objective functions. In this work, the objective functions are defined as the maximum of W and the positive value of minimum of W , i.e. -[minimum of W] for wrinkles deflecting downwards, and \bar{f}_i is a reference value.

The formulation of the design variables and the constraint function in this min-max problem are identical to those of the single-objective optimization problems formulated above. This multi-objective optimization problem is solved in Altair HyperStudy 11.0 using the bound formulation. The problem expressed in Eq. (9) is thus replaced by a conventional optimization problem with an additional design variable β :

minimize β

subject to the original and additional constraints:

$$\frac{f_i(x)}{\bar{f}_i} \leq \beta \quad (10)$$

$$g(x) = g(x_1, x_2, \dots, x_n) \leq 100\% \quad (11)$$

and

$$x_n^L \leq x_n \leq x_n^U \quad (12)$$

where n is the number of design variables in the original minmax problem.

4 Gradient-based shape optimization

Gradient-based optimization techniques is a popular class of optimization methods. These algorithms can be advantageous in simulation-based optimization since the algorithms tend to find an optimum in fewer function evaluations when compared to other techniques. Thus, the Sequential Quadratic Programming (SQP) method implemented in Altair HyperStudy 11.0 was chosen to perform the shape optimization of the corner reinforcement patches.

Tables 3 - 6 summarize the optimum designs of the patches found by solving the single-objective problems formulated in the previous section. The objective functions are:

- (i) maximum of W
- (ii) maximum of $|W|$
- (iii) root mean square (RMS) of W
- (iv) p -mean of W for a range of values of parameter p .

			Baseline	Optimum
Objective function	$f(x)_{max}$	nm	92.08	65.30
Design variables	x_1	μm	225	157
	x_2		0	0.74
	x_3		0	-0.19
Constraint function	$g(x)$	%	100	99.90
Maximum $ W $		nm	92.08	66.00

Table 3: Optimization results for objective function of maximum of W

			Baseline	Optimum
Objective function	$f(x)_{abs}$	nm	92.08	65.55
Design variables	x_1	μm	225	163
	x_2		0	0.64
	x_3		0	-0.14
Constraint function	$g(x)$	%	100	99.54
Maximum $ W $		nm	92.08	65.55

Table 4: Optimization results for objective function of maximum of $|W|$

			Baseline	Optimum
Objective function	$f(x)_{RMS}$	nm	12.76	9.73
Design variables	x_1	μm	225	144
	x_2		0	0.98
	x_3		0	-0.41
Constraint function	$g(x)$	%	100	99.54
Maximum $ W $		nm	92.08	96.44

Table 5: Optimization results for objective function of RMS of W

			Baseline				Optimum			
			Parameter p				Parameter p			
			$p = 4$	$p = 6$	$p = 8$	$p = 16$	$p = 4$	$p = 6$	$p = 8$	$p = 16$
Objective function	$f(x)_{p\text{-mean}}$	nm	26.17	35.98	43.08	59.09	18.14	25.04	29.71	41.33
Design variables	x_1	μm		225			153	163	151	168
	x_2			0			0.80	0.64	0.81	0.57
	x_3			0			-0.22	-0.14	-0.17	-0.10
Constraint function	$g(x)$	%		100			100	99.94	100	100
Maximum $ W $		nm		92.08			65.80	65.54	66.70	66.17

Table 6: Optimization results for objective function of p -mean of W

The solution of the minmax problem using the bound formulation is presented in Table 7.

			Baseline	Optimum
Objective function	$f(x)_{max}$	nm	92.08	44.02
	$f(x)_{min}$		87.09	47.17
Design variables	x_1	μm	225	257
	x_2		0	-0.40
	x_3		0	0.77
Constraint function	$g(x)$	%	100	99.68
Maximum $ W $		nm	92.08	47.17

Table 7: Optimization results for minmax problem formulation

The maximum $|W|$ criterion is more stringent in the sense that it looks at the worst peaks, i.e. maximum wrinkle amplitudes, rather than just the positive ones. In many cases the wrinkle details, such as wavelength and amplitude, are not uniformly distributed through the membrane. The wrinkling intensity strongly depends on the material nonlinearity, boundary conditions and loading because wrinkling occurs due to local instability, that is, when compressive stresses appear anywhere in a membrane. Due to symmetry in geometry, boundary conditions and loading, the wrinkle amplitudes are expected to be fairly symmetric with respect to the positive and negative peaks. The optimization problem formulation to minimize the maximum of $|W|$ can hence provide a benchmark approach to the rest of the approaches can be compared. However, this approach has to be used with care as, generally, gradient-based optimization techniques may exhibit poor convergence for non-smooth function such as $|W|$.

From the Tables 3-6 one can see that the worst quality of the solution is obtained with the RMS criterion giving unexpectedly large wrinkle amplitude of 96.44 nm (Table 5). RMS is used to measure the surface accuracy in many kinds of high-precision structures, where it defines the deviations from the nominal surface. In our

case, the membrane nominal surface is assumed to be perfectly flat in the xy -plane, i.e. $z = 0$. It can be concluded that even though the RMS value of the surface deflection was at a minimum, the deviations were not uniformly distributed and some large deviations existed.

By varying the parameter p from 4 to 16 in Table 6, only a small difference in the solutions was found. It can be seen that the solution using this formulation depends on the value of parameter p but in a rather limited way. Parameter $p = 6$ produces a better solution with respect to maximum $|W|$ compared to p taken as 4, 8 or 16. Generally, it is recommended that, when a generalized mean is used, one has to take the value of parameter p as large as possible to approach the value of maximum $|W|$, see [9] still dealing with a smooth objective function rather than non-smooth maximum $|W|$ function. However, it was observed that for the high values of p the optimization convergence becomes oscillatory and the constraint violation increases. Interestingly, the solution with the parameter $p = 6$ shows a good agreement with the solution by the formulation of minimizing the maximum of $|W|$, as shown in Table 4.

The problem formulation using the minmax formulation yields the best solution, with the maximum of $|W|$ as low as 47.17 nm that has not been found by the rest of the problem formulations. The min-max optimization in fact aims at improving the worst case scenario, that is, the difference between the positive and negative peaks. Whether or not this problem formulation provides a robust solution compared to others will be addressed later in this section.

The common point in all these solutions share is the thickness reduction of the patches, except for the minmax formulation. This indicates that the shape of the patches is the key factor in minimizing the intensity of wrinkles in the corners subjected to tension forces. Figure 8 shows the optimum shape of the patches that corresponds to the p -mean formulation with $p = 6$. The optimum shape of the patches, i.e. blue shaded area, overlays the meshed shape of the baseline design which shows an increase in the total surface area of the patches. This also means that the first shape variable (the curve ratio alteration) plays a more important role than the other in the shape optimization of the patches that corresponds to minimization of the wrinkling of the membrane.

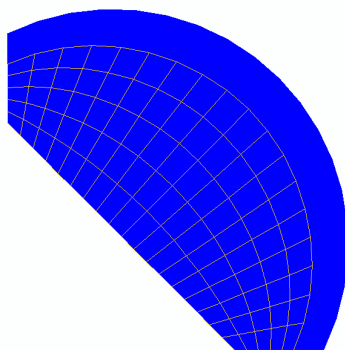


Figure 8: Optimum patch shape compared to the baseline shape (meshed)

As seen in Figure 9, the optimum shape design of the patches results in wrinkles having noticeably lower amplitudes and a fairly symmetric wrinkle profile, i.e. positive and negative amplitudes. This may be due to the increase in the total surface area of the patches as well as the shape of them that unifies the tension lines radiating from the corners where the loads are applied.

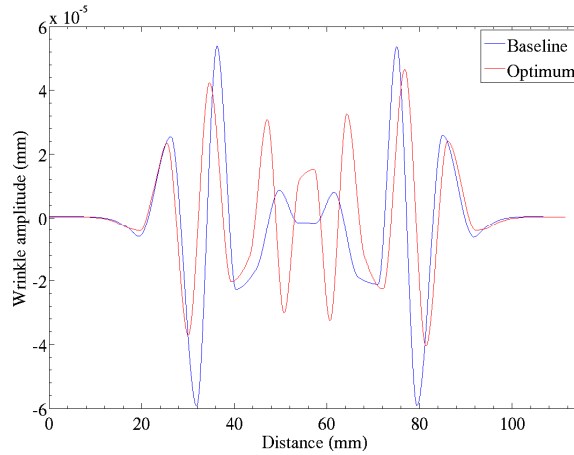


Figure 9: Comparison of the wrinkle profiles for the optimum p -mean ($p = 6$) and the baseline design

Figure 10(a) and (b) show the contour plot of out-of-plane displacement (mm) of the wrinkled membrane and the deformed shape at the distance of 80 mm from the corner. When compared to Figure 4, one can see that the wrinkles at the centre are of much smaller amplitude.

The stress distributions are essentially identical to the baseline design however, it was found to have a slight decrease of high stress concentration in the vicinity of the patches due to the reduction in the thickness.

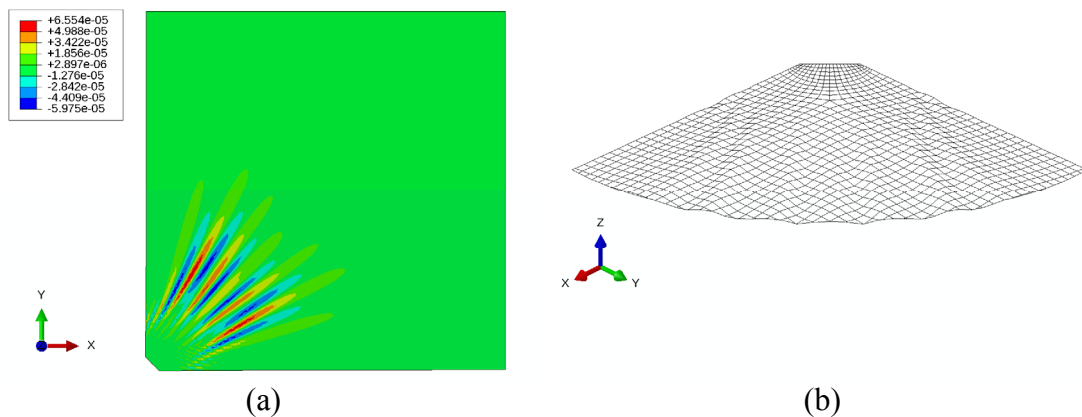


Figure 10: Wrinkle pattern at optimum design for p -mean, $p = 6$: (a) contour of out-of-plane displacement, and (b) wrinkle profile

Figure 11 shows the objective function convergence history for the p -mean ($p = 6$) and minmax formulations. It can be seen that the p -mean formulation produces a steady convergence whereas the minmax formulations shows dramatic jumps in the objective function value. However, it was found that the p -mean formulation took slightly more iterations to converge as compared to others.

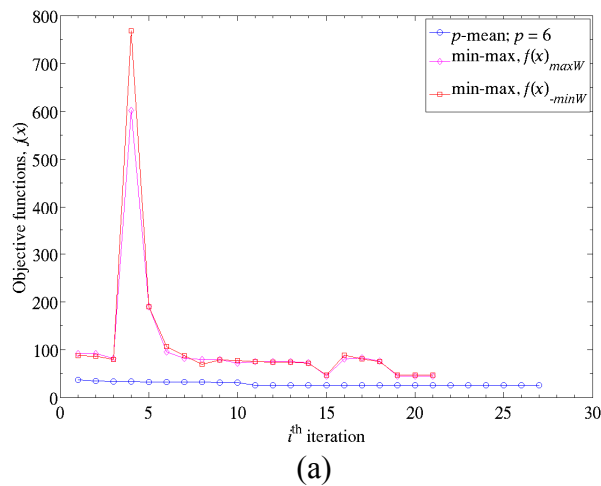


Figure 11: Convergence history plots

It is well-known that the convergence of gradient-based optimization algorithms in the presence of numerical noise is not assured, hence the issue of numerical noise in the function value, maximum of $|W|$, was also examined. One of the design variables, the shape factor x_2 , was incremented by very small amounts as shown in Figure 12 for the optimum design found by the p -mean ($p = 6$) formulation. It can be seen that in the vicinity of the obtained design the function of maximum of $|W|$ is smooth.

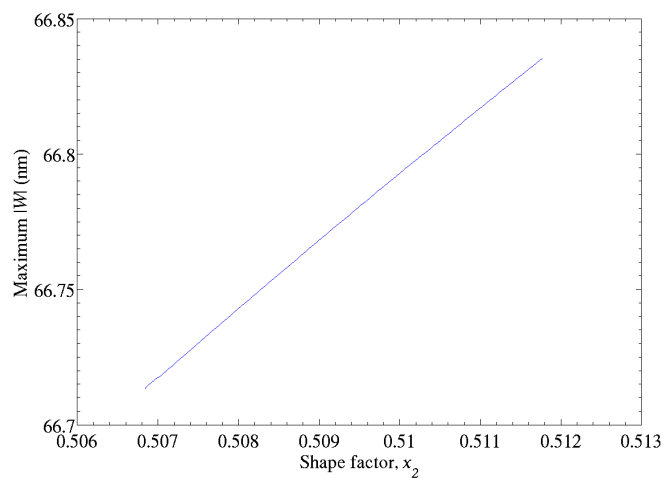


Figure 12: Numerical noise

To check the robustness of the obtained solutions with respect to small perturbations of the inputs, the design variables were incremented by ± 0.01 at the optimum design for each formulation, as shown in Tables 8 and 9. These tables present an indication of the variation of design performance of the patches. It can be seen that small variations of the design variables do not affect the model responses drastically for the case of the p -mean ($p = 6$) formulation. However, they do for the case of minmax formulation. This indicates that the design optimization using the minmax formulation produced a non-robust solution that dramatically deteriorates when the design variables are changed by even a small amount.

	Design variables			Model responses		
	x_1 mm	x_2	x_3	Maximum $ W $ nm	p -mean; $p = 6$ nm	RMS W nm
-0.01	0.15			74.11	30.88	10.63
Optimum	0.16	0.64	-0.14	65.54	25.04	8.56
+0.01	0.17			66.30	25.05	8.58
-0.01		0.63		73.43	30.67	10.59
Optimum	0.16	0.64	-0.14	65.54	25.04	8.56
+0.01		0.65		65.95	25.04	8.56
-0.01			-0.15	73.07	30.67	10.59
Optimum	0.16	0.64	-0.14	65.54	25.04	8.56
+0.01			-0.13	66.25	25.08	8.58

Table 8: Robustness analysis of p -mean formulation ($p = 6$) solution

	Design variables			Model responses		
	x_1 mm	x_2	x_3	Maximum $ W $ nm	p -mean; $p = 6$ nm	RMS W nm
-0.01	0.25			77.73	24.91	6.56
Optimum	0.26	-0.40	0.77	47.17	16.03	4.09
+0.01	0.27			87.56	29.16	8.06
-0.01		-0.41		83.72	28.12	8.00
Optimum	0.26	-0.40	0.77	47.17	16.03	4.09
+0.01		-0.39		71.93	23.93	6.36
-0.01			0.76	81.51	27.62	7.98
Optimum	0.26	-0.40	0.77	47.17	16.03	4.09
+0.01			0.78	72.37	24.64	6.50

Table 9: Robustness analysis for minmax formulation solution

5 Conclusions

Several formulations of the optimization problem of reducing the amplitude of wrinkles on membranes by the shape optimization of the corner reinforcement patches were evaluated and compared. The morphing technique using the

HyperMorph module in Altair HyperMesh 11.0 proves its capability for introducing rapid changes in the mesh shapes while preserving the mesh quality.

Even though the minmax formulation produced the best solution in terms of maximum of $|W|$, the performance of the solution deteriorated quite dramatically when the design variables varied by a small amount indicating the non-robustness of the obtained solution and hence this formulation is not recommended. This and other formulations that include operations of maximum and/or absolute value of the out-of-plane displacement should be used with care as convergence of a gradient-based technique can suffer in such cases.

The p -mean formulation where the parameter p was taken as 6 produced the maximum of $|W|$ of 29% lower than that of the baseline design. This formulation was found to be superior to other problem formulations, it provides an optimization problem with a smooth objective function, a steady convergence history when solved by SQP and robust properties of the obtained design with respect to the small perturbations of the design variables.

References

- [1] E.-J. Yoo, J.-H. Roh, and J.-H. Han, "Wrinkling Control of Inflatable Booms Using Shape Memory Alloy Wires, Smart Materials and Structures, 16(2007), 340-348, 2007.
- [2] L. Zheng, "Wrinkling of Dielectric Elastomer Membranes", PhD Dissertation, California Institute of Technology, United States of America, 2009.
- [3] J. Leifer, J. T. Black, W. K. Belvin, and W. Behun, "Evaluation of Shear Compliant Borders for Wrinkle Reduction in Thin Film Membrane Structures", 2003, AIAA Paper 2003-1984.
- [4] H. Sakamoto, K. C. Park, and Y. Miyazaki, "Evaluation of Membrane Structure Designs Using Boundary Web Cables for Uniform Tensioning", Acta Astronautica, 60(2007), 846-857, 2006.
- [5] C. G. Wang, L. N. Mao, X. W. Du, and X. D. He, "Influence Parameter Analysis and Wrinkling Control of Space Membrane Structures", Mechanics of Advanced Materials and Structures, 17, 49-59, 2010.
- [6] N. Kogiso, K. Toyama, and T. Akita, "Wrinkle Intensity Minimization Design of Space Membrane Structures", Proceedings 12th AIAA/ISSMO Multidisciplinary Analysis & Optimization Conference, Victoria, British Columbia, Canada, 2008, AIAA-2008-6030.
- [7] R. Orszulik, J. Shan, and M. Stachowsky, "Membrane Structure Active Flatness Control Using Genetic Algorithm with Online Objective Reweighting", Acta Astronautica, 68(2011), 2012-2014, 2010.
- [8] Y. W. Wong and S. Pellegrino, "Wrinkled Membranes Part III: Numerical Simulations", Journal of Mechanics of Materials and Structures, 1(1), 61-93, 2006.
- [9] P. Duysinx and O. Sigmund, "New Developments in Handling Stress Constraints in Optimal Materials Distribution", 1998, AIAA 98-4906.

- [10] N. Olhoff, "Multicriterion Structural Optimization via Bound Formulation and Mathematical Programming", *Structural Optimization*, 1, 11-17, 1989.
- [11] N. Olhoff, "On Optimum Design of Structures and materials", *Meccanica*, 31, 143-161, 1996.